

Enhancing Action Recognition by Leveraging the Hierarchical Structure of Actions and Textual Context

Manuel Benavent-Lledo^{a,*}, David Mulero-Pérez^a, David Ortiz-Perez^a, Jose Garcia-Rodriguez^a, Antonis Argyros^b

^a*Department of Computer Technology, University of Alicante, Alicante, Spain*

^b*Institute of Computer Science, FORTH, Heraklion, Crete, Greece*

Abstract

The sequential execution of actions and their hierarchical structure consisting of different levels of abstraction, provide features that remain unexplored in the task of action recognition. In this study, we present a novel approach to improve action recognition *by exploiting the hierarchical organization of actions and by incorporating contextualized textual information, including location and prior actions to reflect the sequential context*. To achieve this goal, we introduce a novel transformer architecture tailored for action recognition that utilizes both visual and textual features. Visual features are obtained from RGB and optical flow data, while text embeddings represent contextual information. Furthermore, we define a joint loss function to simultaneously train the model for both coarse and fine-grained action recognition, thereby exploiting the hierarchical nature of actions. To demonstrate the effectiveness of our method, we extend the Toyota Smarthome Untrimmed (TSU) dataset to introduce action hierarchies, introducing the *Hierarchical TSU dataset*. We also conduct an ablation study to assess the impact of different methods for integrating contextual and hierarchical data on action recognition performance. Results show that the proposed approach outperforms pre-trained SOTA methods when trained with the same hyperparameters. Moreover, they also show a 17.12% improvement in top-1 accuracy over the equivalent

*Corresponding author.

Email addresses: `mbenavent@dtic.ua.es` (Manuel Benavent-Lledo), `dmulero@dtic.ua.es` (David Mulero-Pérez), `dortiz@dtic.ua.es` (David Ortiz-Perez), `jgarcia@dtic.ua.es` (Jose Garcia-Rodriguez), `argyros@ics.forth.gr` (Antonis Argyros)

fine-grained RGB version when using ground-truth contextual information, and a 5.33% improvement when contextual information is obtained from actual predictions.

Keywords: Action Recognition, Action Hierarchies, Action Context, Vision-Language Transformer

1. Introduction

Action recognition has become a fundamental task in a wide range of real-world applications. It involves the understanding of actions occurring within video sequences, allowing for diverse applications in everyday scenarios such as video surveillance [1], autonomous driving [2, 3], and human-robot interaction [4].

In some of these cases, the effectiveness of the provided solutions depends on their ability to operate online and in real-time. However, in several other cases (*e.g.* routine analysis [5, 6]), offline analysis of behavior is sufficient. In such cases, the consideration of the broader context provided by the entire video, may lead to improved model performance.

In the offline setting, action recognition and action detection emerge as the primary tasks in analyzing trimmed and untrimmed videos, respectively. Action recognition involves categorizing videos into predefined classes [7, 8], whereas action detection extends this by identifying the temporal boundaries of each action within the video [9, 10]. While the former pursues a straightforward goal, the latter benefits from the sequential nature of actions to enrich the temporal context, thereby reinforcing the robustness of the model.

The definition of the different action categories is typically left to the discretion of dataset authors, resulting in varying levels of abstraction. For example, the task of *making coffee* may be decomposed into several steps involving different objects: *open coffee maker*, *place filter*, *etc.* While the coarse granularity is sufficient in some cases, certain applications may require additional refinement to achieve specific goals. For example, robotic applications often need more detailed annotations, including per-joint instructions.

This work presents an action recognition architecture that exploits both the hierarchical structure and the sequential execution of actions. To this end, we adopt a transformer encoder built upon state-of-the-art methods [11, 12, 13] that use this architecture to model temporal dependencies. By exploiting the self-attention mechanism inherent in transformer architectures,

this model exceeds previous methods such as 3D CNNs [14, 15, 16] and RNNs [17, 18, 19], which often face challenges in capturing long-range temporal dependencies.

The Transformer architecture [20], originally designed for natural language processing, has undergone numerous improvements in recent years [21, 22, 23]. These improvements have enabled the models to handle temporal dependencies more effectively, and capture contextual information within textual data. We explore the benefits of these models to incorporate contextual data for action recognition in two different ways: (1) evaluating the effect of rephrasing to enrich textual descriptions of past actions along with camera location information leveraging instructional models such as GPT-3.5 [21] and Llama 3 [24]; and (2) encoding textual data into feature vectors using transformer text encoders [23, 25]. By fusing contextual information in the form of text embeddings with visual features prior to classification, we improve the overall representation of the ongoing action, enabling for more accurate action recognition.

Finally, we train our model with a dual objective: coarse-grained and fine-grained action classification. The rationale behind this approach is rooted in the notion that learning together the coarse- and the fine-grained action facilitates the recognition of both. Previous studies [26, 27] have explored action hierarchies under the premise that hyperbolic geometry naturally encodes hierarchical structures. Other works [28, 29] exploit the goal of the video, *i.e.* a coarse-grained action, to improve action anticipation performance. In our method, we propose a joint loss function to allow the model to better discriminate fine-grained actions. For experimentation, we extend the existing Toyota Smarthome Untrimmed (TSU) dataset [30], incorporating action hierarchies into Activities of Daily Living (ADL). Code and extended annotations resulting in the Hierarchical TSU dataset will become publicly available on Github¹.

In summary, the contributions of this paper are the following:

- We introduce a novel vision-language transformer architecture that exploits hierarchical and contextual information from actions to improve accuracy in the task of action recognition. Our approach outperforms state-of-the-art visual-only models.

¹<https://github.com/3dperceptionlab/HierarchicalActionRecognition>

- We present the Hierarchical TSU dataset, an extension of the original TSU dataset [30], incorporating coarse-grained annotations and enriched textual information. Additionally, we compare various strategies for generating textual descriptions of contextual data by leveraging previous actions and camera location.
- We conduct extensive experiments to demonstrate the effectiveness of our approach and to compare it with relevant state of the art methods. Additionally, we present detailed ablation studies that analyze the contributions of our model’s components, as well as the impact of hierarchical and contextual information.

The remainder of the paper is structured as follows. Section 2 summarizes the latest related works. In Section 3 we describe in detail the proposed method. The experiments and results are reported in Section 4, followed by an ablation study in Section 5. Finally, the main conclusions of this work are presented in Section 6.

2. Related Work

We present an overview of pertinent literature concerning action recognition, focusing on the integration of language models and hierarchical structures of actions as tools to enhance performance.

2.1. Action Recognition

Action recognition involves the classification of the action class performed within a video clip. Over time, various methodologies have been devised, with 2D CNN methods relying on single-frame human-object interaction being deemed the least effective due to their lack of temporal context [31]. Temporal modeling stands as a crucial aspect of action recognition. While recurrent neural networks and 3D CNN based methods held sway for several years [14, 15, 16, 17, 18, 19, 32], the advent of video transformers [11, 12, 13] has significantly enhanced temporal modeling capabilities.

Two primary categories of architectures emerge. The first one comprises end-to-end models such as ViVit [33] which uses a pure transformer architecture for video classification inspired by the advances in the image domain. Embeddings are extracted as non-overlapping tubelets that span both the spatial and temporal dimensions. In TimeSformer [34], a convolution-free

approach was presented with a detailed study on self-attention schemes. Results from this study suggest that divided attention for spatial and temporal features leads to the best performance. Video Swin [35] explores the inductive bias of locality in video transformers by adapting the Swin transformer designed for the image domain [36]. MViT [37] employs multiscale feature hierarchies with a pyramid of feature activations, allowing effective modeling of simple low-level, and complex high-level visual information. MViTv2 [38] enhances its predecessor with decomposed relative positional embeddings and residual pooling connections.

Second, temporal modeling transformers that use pre-trained feature extractors from large datasets such as Kinetics-400 [14] and ImageNet [39]. OadTR [11] focus on temporal modeling using decoded RGB frames and frozen frame-level feature extractors. In addition, optical flow is computed from the RGB data to improve accuracy. Similarly, TIM [40] uses frozen visual and audio encoders for feature extraction. Features include a timestamp provided by a Time Interval MLP, so that the model can be queried about the events at a given interval in a specific modality. Other approaches incorporate the vision transformer, ViT [41], to fine-tune the feature extractor on the corresponding datasets [7, 8, 42], yielding better results with a remarkable increase in terms of computing cost.

Feature extractors usually consist of 2D or 3D CNNs such as ResNet [43], InceptionV3 [44] or I3D [14]. On the contrary, MM-Vit [13] diverges by operating on multimodal features extracted from compressed videos, including I-frames, motion vectors and audio features. Similar strategies are observed in [45, 46, 47].

2.2. Language Models for Action Recognition

The remarkable capabilities of large language models in temporal modeling and feature representation have been thoroughly investigated [21, 22, 23]. These capabilities have found application in various vision tasks, notably in image and video captioning. While these approaches focus on generating textual descriptions of videos [48], recent research has explored the use of language models to improve action recognition results. For example, ActionCLIP [7] uses a contrastive learning approach inspired by CLIP [49] to improve action recognition. Instead of image captions, action classes are converted to prompts, which are then compared to the aggregated representation of a video. Spatial features from frames are extracted from a fine-tuned version of CLIP’s visual encoder, based on ViT [41]. Similarly,

VideoCLIP [50] extends this learning paradigm to various video understanding tasks. Building on these advances, Text4Vis [8, 42] proposes to initialize a frozen classifier for action recognition using text embeddings derived from language models. Moreover, BIKE [51] introduces a novel framework that facilitates bi-directional cross-model knowledge transfer from vision to language models, with the aim of improving action recognition in videos.

Furthermore, the capabilities of language models in capturing temporal dependencies and contextual understanding have been exploited to model past actions as well [52]. VLMAH [53] presents a visual-linguistic approach to modeling action history that is particularly useful for instructional videos due to the sequential nature of the actions. Similarly, Furnari and Farinella [54] use “rolling-unrolling” LSTMs to succinctly summarize past actions. In contrast, AntGPT [29] exploits large language models for in-context learning [21] long-term action anticipation, *i.e.* by providing few ground-truth examples. Similarly, [55] explores the benefits of incorporating object representations for this task. Encoded representations of cropped objects from RGB frames, along with bounding boxes and object labels encoded as text embeddings, are shown to improve the model’s performance.

2.3. Action Hierarchies

While current action recognition techniques have made significant progress, they often fall short in segmenting actions into distinct phases, which is required for many real-world applications. To address this gap, the authors of the FineGym dataset [56] introduced a sports video dataset with a three-level semantic hierarchy. Previous research [26, 27] has explored this dataset using the premise that hyperbolic geometry inherently encodes hierarchical structures. Using the Poincaré ball, these studies define a distance metric between predictions and observations, where points closer to the center of the ball represent abstract embeddings, while those near the edge denote specific ones. Essentially, edge proximity indicates higher model confidence.

In addition, Timeception [57] redefines the notion of activity, restricting it to “complex actions” characterized by: (1) composition - consisting of several simpler actions, (2) temporal order of these actions, and (3) extent - recognizing the variability in temporal length between actions. By introducing the Timeception layer, the architecture tolerates both long-range temporal dependencies and variations in the temporal extent.

The previously introduced AntGPT [29] also benefits from hierarchical information by incorporating goal information extracted from past actions using a large language model. The resulting text embedding is fused with visual observations to improve long term action anticipation. Similarly, in [28], authors exploit the goal concept to improve action anticipation in industrial scenarios by introducing a consistency loss to ensure alignment between coarse-grained and fine-grained predictions.

It is important to note the scarcity of annotated hierarchical data in the ADL domain, which prompts researchers in [26] to manually extend existing datasets for experimentation. Alternatively, synthetic data generators, such as Virtualhome [58], offer a hierarchical approach to generating video data, providing a valuable resource to address this limitation.

3. Methodology

We present the proposed method for action recognition using hierarchical action structures and textual context. Figure 1 illustrates an overview of the proposed architecture.

3.1. Video Encoder

We adopt a standard Transformer’s encoder to model temporal dependencies as in [11]. Given a trimmed video $V = \{f_t\}_{t=-T}^0$ associated with a coarse-grained action, and one or more fine-grained actions, the frames f_t are grouped into blocks of size B , resulting in $(T + 1)/B$ chunks. For each block, we use a frozen feature extractor to obtain spatial features from RGB and optical flow frames, and employ separate video encoders with the same structure for each modality. We use the central frame of the block for RGB features, and the B frames sequence for optical flow features. These features are mapped into a D dimensional feature space, which we can formalize as $F = \{\mathcal{O}_t\}_{t=-T}^0 \in \mathbb{R}^{(T+1) \times D}$, where \mathcal{O}_t represents the output token of the transformer encoder at time t .

We extend the feature vector with an additional learnable class token with $\mathcal{O}_{CLS} \in \mathbb{R}^D$. This token is used to learn the aggregated representation of the entire input, and is combined with the feature sequence as $\hat{F} = \text{Stack}(\{\mathcal{O}_t\}_{t=-T}^0, \mathcal{O}_{CLS}) \in \mathbb{R}^{(T+2) \times D}$. Alternatively, the aggregated representation of the input can be obtained as the mean of the tokens in the input sequence as in [59].

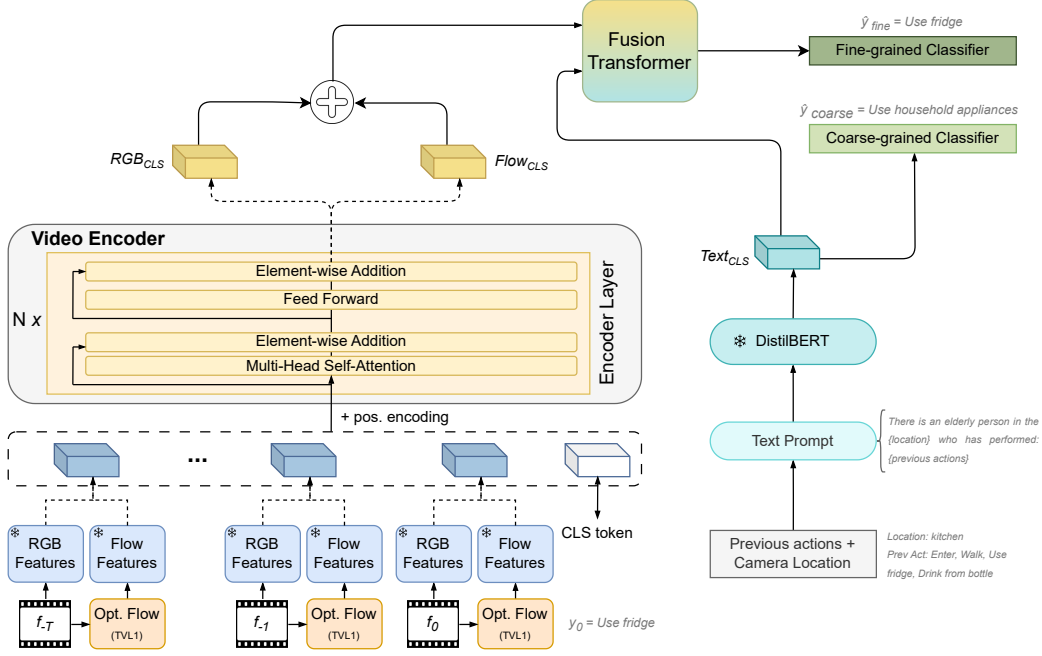


Figure 1: **Overview of the proposed action recognition architecture.** From a video input, frozen feature extractors obtain spatial features from RGB frames and temporal motion features from optical flow. These features, along with a class token, are processed through individual video transformer encoders for each visual modality, capturing long-range temporal dependencies. Dashed lines indicate the use of either RGB or flow features and their respective embeddings, though only a single video encoder is depicted for simplicity. Additionally, DistilBERT extracts textual features that represent the current location and previous actions. Coarse-grained actions are recognized based on contextual information, specifically utilizing the textual embeddings while the fine-grained classifier leverages the fused features from the fusion transformer.

Due to the lack of frame positional information in the encoder, we additionally embed positional encodings. Experiments comprise fixed sinusoidal inputs and trainable embeddings. We add positional encoding $E_{pos} \in \mathbb{R}^{(T+2) \times D}$ as shown in Equation 1, *i.e.*, an element-wise addition to preserve positional information:

$$X_0 = \hat{F} + E_{pos}. \quad (1)$$

The fundamental element of the transformer model is the multi-head self-attention (MSA) mechanism. In essence, self-attention enables each token to engage with others, enhancing its ability to gather valuable semantic insights.

This process involves calculating dot products between queries and keys, followed by a softmax function to determine the importance assigned to each value. Formally,

$$X' = Norm(X_0), \quad (2)$$

$$Attention(Q_i, K_i, V_i) = softmax\left(\frac{Q_i K_i^T}{\sqrt{d_k}}\right) V_i, \quad (3)$$

$$H_i = Attention(Q_i, K_i, V_i), \quad (4)$$

where $Q_i = X'W_i^q$, $K_i = X'W_i^k$ and $V_i = X'W_i^v$ are linear layers applied to the input sequence, $W_i^q, W_i^k, W_i^v \in \mathbb{R}^{D \times \frac{D}{N_{head}}}$ with N_{head} represent the number of heads, and $\frac{1}{\sqrt{d_k}}$ is a scaling factor that helps stabilizing the training and speed up convergence. Note that queries, keys and values are all vector representations. The outputs of each head are concatenated and fed into a linear layer as:

$$\hat{H} = Stack(H_1, H_2, \dots, H_{N_{head}})W_d \in \mathbb{R}^{(T+2) \times D}, \quad (5)$$

where W_d is a linear projection.

Finally, the output is fed into a two-layer feed-forward network (FFN) with GELU activation. Meanwhile, layer normalization and residual links are also applied. The video encoder formulas can then be summarized as follows:

$$\hat{H} = MSA(Norm(X_0)), \quad (6)$$

$$m'_1 = \hat{H} + X_0, \quad (7)$$

$$m_n = FFN(Norm(m'_{n-1})) + m'_{n-1}, \quad (8)$$

$$m'_n = MSA(Norm(m_{n-1})) + m_{n-1}, \quad (9)$$

where $n \in N$ is the n -th encoder layer with a total of N , m' denotes the output of the first element-wise addition in the encoder layer and $m_N \in \mathbb{R}^{(T+2) \times D}$ is the final feature representation of the last encoder layer. For the remaining of the paper, and for simplicity, we use $m_{CLS} \in \mathbb{R}^D$ to denote the output representation of the class token from an encoder. This notation is extended to m_{RGB} and m_{Flow} to refer to the same token of the corresponding modality.

3.2. Contextualized Textual Information

Large language models have shown exceptional abilities in temporal modeling and understanding context. To leverage these capabilities, we propose an approach that models past information to enhance the contextualization of current action recognition. Specifically, given the location and N previous actions, we use a prompt (as illustrated in Figure 1) to provide context about prior events, thus modeling longer temporal dependencies. From the generated sentences, we extract feature vectors using DistilBERT [25], a distilled variant of BERT [23], which employs deep bidirectional transformer encoders for text comprehension. As for the video encoder, we utilize the class token to represent the entire input sequence, denoted as m_{Txt} .

In addition to DistilBERT, we compare its performance against BERT and explore the use of LLMs for rephrasing to increase variability and enrich the data. Section 5 presents results for different setups, including no rephrasing, and rephrasing using GPT-3.5 [21] and Llama 3 [24], as well as an analysis of the optimal number of past actions and the impact of location information on contextualization.

3.2.1. Exploiting Hierarchical Information from Context

Contextual information derived from past actions and location provides a general understanding of the ongoing action, effectively yielding a coarse-grained representation. Likewise, this coarse-grained action can serve as supplementary supervision, enhancing fine-grained action recognition performance. To leverage this relationship, we introduce a coarse-grained classifier, which, in conjunction with a joint loss function, improves the accuracy of fine-grained action recognition.

3.2.2. Fusion of Visual and Textual Embeddings

In addition to their capabilities in temporal aggregation, transformer architectures excel at fusing features from different modalities [60]. To leverage this advantage, we employ a transformer encoder to combine visual and textual embeddings. Specifically, we concatenate RGB and optical flow features, as this approach has shown improved performance compared to feeding them separately into the fusion transformer. The encoder layers are structured similarly to the video encoder, but without the class token or positional encoding. Formally,

$$m_{VIS} = m_{RGB} + m_{Flow}, \quad (10)$$

$$m_M = \text{FusionTransformer}(m_{VIS}, m_{Txt}), \quad (11)$$

where $m_{VIS} \in \mathbb{R}^{2 \times D}$ represents the combined RGB and optical flow features which are then mapped to the embedding space of the fusion transformer, denoted as \hat{D} . The output $m_M \in \mathbb{R}^{2 \times \hat{D}}$ results from the M layer of the fusion transformer. The final representation from the fusion transformer, obtained as the mean of the output tokens, is denoted as m_{Fus} .

3.3. Training

The model is trained on a dual classification objective. First, a fine-grained classifier uses m_{Fus} as input. Second, a coarse-grained classifier leverages contextual information from m_{Txt} . The resulting logits from both classifiers are used for multi-class classification, given the existing overlaps between composite actions, as discussed in the next section.

The supervision of both fine-grained and coarse-grained actions is performed through a joint loss function, defined as:

$$\mathcal{L} = BCE(\sigma(z_{coarse}), y_{coarse}) + BCE(\sigma(z_{fine}), y_{fine}), \quad (12)$$

where z and y represent predicted logits and ground truth labels, respectively. The function BCE denotes the binary cross-entropy loss, and σ is the sigmoid activation function applied to the logits. Using this combined formulation ensures numerical stability by applying the sigmoid and binary cross-entropy operations together, rather than separately.

4. Experiments

We now present the experimental setup on the Hierarchical TSU dataset. The results demonstrate the effectiveness of the proposed method compared to the equivalent visual-only approach, and state-of-the-art methods.

4.1. Hierarchical TSU Dataset

The experimental framework in this work is built upon the Hierarchical TSU dataset, a hierarchical dataset for activities of daily living, which extends the Toyota Smarthome Untrimmed (TSU) dataset [30]. The proposed dataset emphasizes the use of contextual information for action recognition,

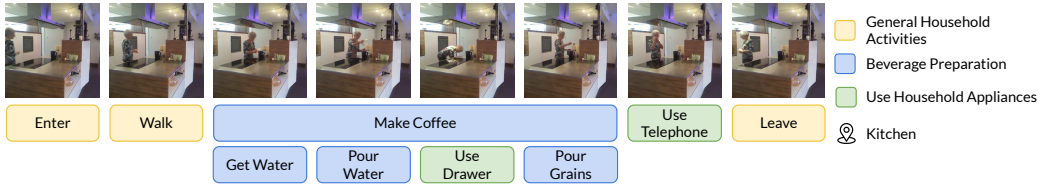


Figure 2: **Example of annotations in the Hierarchical TSU dataset.** Video frames are labeled with fine-grained classes, such as composite activities (e.g., *Make coffee*). Each color represents a coarse-grained activity corresponding to its associated fine-grained class.

in contrast to the TSU dataset designed for action detection, and the original Toyota Smarthome dataset [61], which features short videos of individual actions with limited contextual information and a narrower number of classes.

The TSU dataset provides a rich variety of subjects and spatial settings within a home. With 51 different activity categories, it provides a comprehensive representation of daily living tasks. The dataset is captured by 7 static cameras at known locations, which provide additional contextual data. The combination of these cameras with the dense annotations provided for the untrimmed videos, makes this dataset a suitable option for our problem. In total, the dataset consists of 536 untrimmed videos with an average duration of 21 minutes. The videos capture the daily activities of 18 individuals aged between 60 and 80.

Among the 51 classes, we find elementary actions such as *walk* or *get water*, and composite ones that may overlap with the elementary ones, like *make coffee* or *cook*. Despite the hierarchical relationship between some composite and elementary classes, we maintain the original 51 classes from the TSU dataset and introduce a higher-level hierarchy comprising all action classes. We categorize these actions into 7 coarse-grained action categories based on the contextual meaning, location, and visual similarities, resulting in the Hierarchical TSU dataset. Each of the 51 categories is associated with one of the following classes: *beverage preparation*, *general household activities*, *cleaning*, *prepare breakfast*, *use household appliances*, *cook* and *drink*.

Action segments corresponding to action detection annotations are processed for contextual action recognition. From untrimmed annotations, each trimmed video corresponds to the duration of a fine-grained action segment, with possible overlaps both in fine- and coarse-grained actions due to composite activities, as depicted in Figure 2. Additionally, we process the se-

quence of previous actions to include longer temporal dependencies, which are treated as textual information. Finally, since the location of the fixed cameras is known and detailed in [30], we also include the location of the action as additional contextual information.

4.2. Experimental Setup

Evaluation: We evaluate the results of our experiments on top- k accuracy following previous work on action recognition [7, 8, 61]. Top- k accuracy measures how often the correct action label appears among the top- k labels predicted by the model. We use the cross-subject evaluation introduced in the TSU dataset [30], which uses 11 subjects for training and the remaining 7 for testing. Unless specified otherwise, in all tables, the best performance is highlighted in bold, and the best performance within each subgroup, if applicable, is underlined.”

Implementation details: After exhaustive ablation experiments to determine the best configuration, we adopt ViT-H [41] with a patch size of 14 as RGB feature extractor and Inception v3 [44] from the two-stream network TSN [62] for optical flow features. TLV1 algorithm is used to compute optical flow frames. To extract embedding vectors from textual data we use DistilBERT [25].

The video encoder is composed of 4 attention layers with a single attention head, and an embedding size of 2048. The input vector is supplemented with learned position encoding and a CLS token. The resulting RGB and optical flow video embeddings are concatenated, and this visual representation is fused with text embeddings using the fusion transformer composed of 2 encoder layers, with 2 attention heads per layer and an embedding size of 768. The best performance is obtained using 32 blocks as input, which corresponds to 6.4 seconds of video. The prompt for contextual information contains 5 past actions along with location data.

Training details: The proposed method is implemented using PyTorch, and all experiments are conducted on Nvidia RTX 4090 GPUs. We employ AdamW optimizer with a weight decay of 0.1 and a base learning rate of 5×10^{-5} . Models are trained for 100 epochs with a batch size of 32, employing an early stopping mechanism with a patience of 20 epochs. We use gradient clipping to avoid exploding gradients and warm up the learning rate for 5 epochs. We set the block size to 5, which implies a downsampling rate of 5 on the 25 fps videos from the TSU dataset.

Table 1: Comparison of results: input modalities and joint loss on the best settings.

Modalities	Joint Loss	Fine-Grained		Coarse-Grained	
		Top-1	Top-5	Top-1	Top-5
RGB	-	37.83	72.69	-	-
	✓	<u>38.27</u>	73.55	75.62	99.41
Flow	-	39.09	72.69	-	-
	✓	<u>39.39</u>	69.95	75.18	99.07
RGB + Flow	-	39.90	72.66	-	-
	✓	<u>40.24</u>	74.21	75.44	99.37
RGB + Text	-	53.43	84.03	-	-
	✓	<u>54.80</u>	84.37	75.77	99.37
Flow + Text	-	50.83	79.44	-	-
	✓	<u>50.91</u>	81.07	75.29	99.56
RGB + Flow + Text	-	53.98	84.36	-	-
	✓	54.95	84.11	73.77	99.15

4.3. Results

To determine the best combination of visual input with contextual data that provides the best top- k accuracy, Table 1 contains the results for the best settings obtained after extensive ablation experiments (see Section 5).

For each experiment, we evaluate using both a fine-grained only training objective (-), and a dual training objective with the proposed joint loss (✓). The results lead to the conclusion that the proposed method outperforms the standard approach relying only on visual inputs. Moreover, for every input combination it is observed that predicting both fine- and coarse-grained actions results in better performance. Note that the observed decrease in top-5 accuracy in some cases is primarily due to the model’s high confidence in the top classes.

Impact of optical flow on video analytics: Optical flow is considered an auxiliary modality that complements RGB data, providing a notable performance boost of 1.97% when used in combination with RGB, and even outperforming in the uni-modal approach (1.26%). Although, when combined with contextual information, its effectiveness diminishes, underperforming compared to the corresponding RGB-based method. When all three modalities (RGB, optical flow, and contextual information) are combined, optical

Table 2: Action recognition performance when contextual data are obtained from predictions.

Modalities	Fine Grained		Coarse Grained	
	Top-1	Top-5	Top-1	Top-5
RGB + Text	40.35	71.92	70.88	98.04
Flow + Text	41.42	70.99	70.43	97.85
RGB + Flow + Text	43.16	71.21	66.54	97.81

flow contributes only a marginal improvement of 0.15%.

On the effect of the joint loss function: Using a joint loss function to predict both fine-grained and coarse-grained actions during training enhances performance across all input modalities. This approach yields up to a 1.37% improvement when fusing RGB and text embeddings. Notably, the top- k performance of the coarse-grained classifier is correlated with improvements in fine-grained action recognition.

On the effect of exploiting contextual data: Contextual data, which includes information about previous actions and location in text format, is dependent on visual observations from past frames. As a result, it is always combined with visual modalities and not used independently. Our results demonstrate that incorporating contextual data significantly enhances performance, yielding a 17.12% improvement compared to the RGB-only fine-grained approach, and outperforming all other fusion combinations.

To further validate the efficacy of the proposed method, we evaluate the best-performing model using contextual data extracted from its own predictions instead of ground truth annotations. Table 2 presents the top- k accuracy for both fine- and coarse-grained actions. The results demonstrate the robustness of the method, even when relying on predicted labels. Compared to the previous joint loss results without contextual data, our method achieves a 2.08% improvement with RGB data, a 2.03% improvement with optical flow data, and a 2.92% improvement with the combined RGB and optical flow approach.

4.4. Comparison with State-of-the-art Methods

To evaluate the reliability and robustness of our proposal, we compare our method with existing state-of-the-art architectures for action recognition. To this end, we train different models initialized to pre-trained Kinetics 400 [14]

Table 3: Comparison to state-of-the-art methods trained on the Hierarchical TSU dataset.

Model	# Input Blocks	Top-1	Top-5
X3D [64]	16	30.22	67.05
MViT (Base) [37]		33.01	70.28
MViTv2 (Small) [38]		32.47	70.80
<u>Ours</u> (Predictions)		<u>37.98</u>	67.55
Ours (Ground Truth)		51.14	81.02
VideoResNet [63]	32	36.72	75.70
SlowFast [32]		36.53	68.77
Video Swin (Base) [35]		36.42	74.18
Video Swin (Small) [35]		37.05	74.32
Video Swin (Tiny) [35]		36.75	70.32
<u>Ours</u> (Predictions)		<u>43.16</u>	71.21
Ours (Ground Truth)		54.95	84.11

weights during 100 epochs, the same number of epochs as the proposed method. 3D CNN models (VideoResNet [63], SlowFast [32] and X3D [64]) are trained with a learning rate of 10^{-4} and Adam optimizer, due to improved performance compared to the the training parameters of transformer based architectures. Such models (Video Swin [35] and MViT [37, 38]) are trained with the same hyperparameters as our model. Table 3 presents the results demonstrating that our model outperforms both 3D CNN and transformer based architectures on the Hierarchical TSU dataset, when trained with the same input size and hyperparameters. In this case the best performance, obtained from ground truth contextual data, is shown in bold. The second-best, derived from predictions, is underlined for each number of input blocks.

5. Ablation Experiments

We present an ablation study to evaluate the contributions of various components of the proposed method. In addition to identifying the optimal RGB feature extractor and determining the best configuration values for the transformers used in the architecture, we compare different methodologies for incorporating hierarchical information. We also conduct an ablation analysis on the influence of the number of past actions and location data within the contextual information. Furthermore, we experiment with GPT-3.5 and

Table 4: Effect of rephrasing and comparison of text feature extractors.

Feature Extractor	Rephrasing	Top-1	Top-5
BERT	GPT 3.5	39.46	73.14
	Llama 3	<u>40.79</u>	75.18
	-	40.53	75.36
DistilBERT	GPT 3.5	48.50	80.47
	Llama 3	49.20	79.84
	-	54.95	84.11

Table 5: Study on the number of past actions and effect of location on contextual data.

# Past Actions	Location	Top-1	Top-5
1	-	49.17	82.33
	✓	<u>50.87</u>	84.25
3	-	<u>52.58</u>	84.29
	✓	51.80	84.70
5	-	53.46	84.18
	✓	54.95	84.11
7	-	<u>52.46</u>	82.33
	✓	50.95	80.81

Llama 3 to investigate the effect of rephrasing on enriching contextual data, as well as the impact of different text encoders. Unless specified otherwise, for the experiments in this section we use the best configuration settings that yield a 54.95% top-1 accuracy, and report results on fine-grained action recognition.

5.1. Contextual Data Analysis

The best performing model considers the last 5 actions and the location provided by fixed cameras as contextual data. Text embeddings are obtained using DistilBERT [25] for feature extraction and the *prompt* used to generate the descriptions is a fixed template. Table 4 compares the use of DistilBERT and BERT as feature extractors as well as the use of rephrasing to enhance textual descriptions exploiting two well known large language models: GPT3.5 and Llama 3.

Results indicate that DistilBERT outperforms its predecessor for feature

Table 6: Comparison of strategies for hierarchical action recognition.

Method	Fine-Grained		Coarse-Grained	
	Top-1	Top-5	Top-1	Top-5
Contextual Data (1)	54.95	84.11	73.77	99.15
Separate Fusion (2)	51.83	82.14	73.10	99.19
Separate Classifier (3)	51.24	81.88	74.21	99.11
Shared Classifier (4)	48.17	78.55	73.18	99.44

extraction. Additionally, a notable improvement is observed when using DistilBERT with a fixed template, as opposed to rephrasing for enhancing textual descriptions. Using the optimal configuration, we conducted a study to determine the best number of past actions and the impact of location on contextual descriptions. The results, presented in Table 5, suggest that five past actions is the optimal value on the Hierarchical TSU dataset. Regarding location information, we observe that it provides improvements only when using 1 or 5 past actions, with variability in other cases.

5.2. Strategies for Hierarchical Action Recognition

We compare various strategies to integrate fine-grained and coarse-grained action recognition into a joint learning scheme. Table 6 contains the results using 4 different mechanisms depending on the features used to disambiguate fine- and coarse-grained information. Specifically, (1) using only contextual information for coarse-grained action recognition. Another set of options is to use both visual and contextual information from the vision transformer, by (2) using two separate fusion transformers and (3) using two separate classifiers from the same fused embeddings. Another option (4) is to share partial layers of the classifier, separating only the last layers for classification.

Results indicate that the degree of differentiation between fine-grained and coarse-grained features significantly affects performance. Specifically, using only contextual information for coarse-grained action recognition (1) achieves the best performance, with a Top-1 accuracy of 54.95% for fine-grained actions and competitive results for coarse-grained actions. This confirms that contextual data alone is optimal for coarse-grained recognition and enhances fine-grained performance.

Table 7: Comparison of fusion strategies.

Method	Top-1	Top-5
Separate Modalities	49.94	80.03
Visual Concat	54.95	84.11
Concat	40.53	74.25

Table 8: Ablation study on the number of encoder layers on the fusion transformer.

# Enc. Layers	Top-1	Top-5
1	54.80	84.81
2	54.95	84.11
3	51.32	81.96
4	50.46	82.07

Table 9: Ablation study on the number of attention heads on the fusion transformer.

# Att. Heads	Top-1	Top-5
1	53.21	83.70
2	54.95	84.11
4	52.02	83.22
6	51.32	82.81
8	53.61	83.70

5.3. Data Fusion

Effective fusion of data modalities is crucial for achieving strong model performance. To this end, we evaluate three different fusion strategies and conduct an ablation study on the most effective one: the fusion transformer. RGB and optical flow features are obtained separately, based on the finding that late fusion is the best strategy for the video encoder, as discussed in the next section. We assess the impact of three approaches: (1) concatenating all three modalities (RGB, optical flow, and text), (2) concatenating the visual modalities (RGB and optical flow) prior to the fusion transformer, and (3) inputting the three modalities separately. Table 7 contains the results, with visual concatenation prior to the fusion transformer performing best on top-1 accuracy.

Since the fusion transformer outperforms the concatenation approach, we conduct an ablation study on the number of attention heads and encoder layers, while keeping the embedding size fixed at 768, which corresponds to the text modality. Table 8 presents the results for different numbers of encoder layers, with two layers yielding the best performance. Similarly, Table 9 shows the results for varying numbers of attention heads, with two heads being the optimal configuration for our method.

Table 10: Ablation study on the number of input blocks.

# Input Blocks	Video duration (sec)	Top-1	Top-5
8	1.8	49.45	80.56
16	3.2	51.14	81.02
32	6.4	54.95	84.11
64	12.8	50.70	84.50

Table 11: Ablation study on RGB features extractors.

Feature Extractor	Top-1	Top-5
Inception v3 [44]	47.57	77.81
BN-Inception [65]	48.54	79.33
ViT-H/14 [41]	54.95	84.11

5.4. Video Transformer

We determine the optimal configuration for the video encoder by evaluating several factors: input length, RGB feature extractor, number of layers and attention heads, fusion strategy, embedding size, and the use of positional encoding and CLS tokens.

Input Length: In theory, longer input sequences should improve action recognition accuracy, provided there is no data loss due to excessively long sequences. Table 10 shows the results of our experiments with different sequence lengths. Our findings indicate that an input length of 6.4 seconds (32 input blocks) yields the best performance. Longer sequences tend to miss specific actions within the dataset, while shorter sequences lack the temporal context needed for accurate recognition.

RGB Feature Extractor: Since transformer models for feature extraction are typically trained on static images rather than videos, they may encounter challenges such as motion blur caused by moving objects or people. To address this, we experiment with ViT-H/14 [41] as well as RGB feature extractors from the two-stream network TSN [62], both using pre-trained weights from the Kinetics dataset [14]. Specifically, we evaluate Inception v3 [44] and BN-Inception [65]. As shown in Table 11, despite being trained on static images, the transformer-based method achieves the best accuracy.

Positional Information: As pointed out in Section 3, extracted frame

Table 12: Ablation study on position encoding

Positional Encoding	Top-1	Top-5
-	44.31	76.33
Fixed	52.21	82.96
Learnable	54.95	84.11

Table 13: Ablation study on the number of encoder layers.

# Enc. Layers	Top-1	Top-5
2	52.76	82.07
4	54.95	84.11
6	54.50	84.18
8	54.76	83.03

Table 14: Ablation study on the number of attention heads.

# Att. Heads	Top-1	Top-5
1	54.95	84.11
2	52.02	81.92
4	44.98	76.58
8	42.91	74.84
16	42.65	75.84

features lack order information. Table 12 contains an ablation study on using fixed and learnable position encodings against not using them. Results show that positional encoding to preserve the order of the frames is necessary, and that learned positional encoding performs best.

Number of Encoder Layers and Heads: Finding a balance between the number of encoding layers and attention heads plays a critical role in the performance of transformer models. In Table 13 results show that 4 encoding layers is the best value for this task. Similarly, Table 14 shows that the model accuracy improves when using a single attention head.

Embedding Size and Visual Fusion Strategy: We experiment with three different embedding dimensions on two visual fusion strategies: early and late. Early fusion involves concatenating feature vectors before the input to the transformer encoder. On the contrary, a late fusion strategy requires two video encoders, one for RGB features and one for optical flow features. The results are shown in Table 15, with late fusion and an embedding size of 2048 providing the best top-1 accuracy.

Encoder Representations: The output of the transformer encoder provides a representation for each input token. To avoid biasing the model towards a particular video block, we experiment with two different represen-

Table 15: Ablation study on the embedding dimension and visual fusion strategies.

Fusion Type	Embedding Size	Top-1	Top-5
Early	768	43.98	73.18
	1024	44.35	75.81
	2048	<u>53.72</u>	83.96
Late	768	45.35	77.36
	1024	45.94	76.47
	2048	54.95	84.11

Table 16: Ablation study on the encoder representation.

Encoder Representation	Top-1	Top-5
CLS token	54.95	84.11
Mean	45.72	78.21

tations as explained in Section 3. As shown in Table 16, using a class token improves the encoder’s representation, resulting in a more robust model compared to the mean of each of the encoder’s output tokens.

6. Conclusion

In this paper, we present a novel approach for action recognition by leveraging the capabilities of language models to generate contextualized representations of previously performed actions and their locations. This enables us to capture the sequential and contextual properties of actions effectively. Additionally, we introduce a joint loss function for both coarse-grained and fine-grained action recognition, benefiting from the hierarchical structure of actions. Our method is built on a transformer encoder for video feature extraction, which incorporates a class token for enhanced representation and positional encoding to preserve the temporal order of input video blocks. We fuse text and video features using a transformer encoder, trained with a dual objective to compute the joint loss.

For our experiments, we extend the TSU dataset by introducing the Hierarchical TSU dataset, which focuses on activities of daily living and emphasizes the hierarchical nature of actions. Despite its simplicity, our method outperforms comparable visual-only methods, including those with the same

architecture and pre-trained state-of-the-art models, when trained under the same hyperparameters.

While future work may explore alternative video aggregation and feature fusion mechanisms, this study focuses on the hierarchical properties of actions by analyzing the effects of various textual prompts, such as the number of previous actions and the relevance of location, using different text encoders. We also evaluate different strategies for incorporating hierarchical information into action recognition.

Acknowledgments

This work has been funded by the Valencian regional government CIAICO/2022/132 Consolidated group project AI4Health, and International Center for Aging Research ICAR funded project “IASISTEM”. This work has also been supported by a Spanish national and two regional grants for PhD studies, FPU21/00414, CIACIF/2021/430 and CIACIF/2022/175.

Statements and Declarations

Conflict of interest. The authors declare that they have no conflict of interest.

Data Availability. The dataset used in the current study is publicly available from the corresponding authors. Extended annotations for the Hierarchical TSU dataset are available at <https://github.com/3dperceptionlab/HierarchicalActionRecognition>.

Code Availability. The code for the presented work has been published on GitHub <https://github.com/3dperceptionlab/HierarchicalActionRecognition>.

References

- [1] P. Ni, S. Lv, X. Zhu, Q. Cao, W. Zhang, A light-weight on-line action detection with hand trajectories for industrial surveillance, *Digital Communications and Networks* 7 (1) (2021) 157–166. doi:10.1016/j.dcan.2020.05.004.
- [2] J. Kim, T. Misu, Y.-T. Chen, A. Tawari, J. Canny, Grounding human-to-vehicle advice for self-driving vehicles, in: *CVPR*, 2019.

- [3] V. Ramanishka, Y.-T. Chen, T. Misu, K. Saenko, Toward driving scene understanding: A dataset for learning driver behavior and causal reasoning, in: CVPR, 2018.
- [4] L. Tong, H. Ma, Q. Lin, J. He, L. Peng, A novel deep learning bi-gru-i model for real-time human activity recognition using inertial sensors, *IEEE Sensors Journal* 22 (6) (2022) 6164–6174. doi:10.1109/JSEN.2022.3148431.
- [5] E. Talavera, C. Wuerich, N. Petkov, P. Radeva, Topic modelling for routine discovery from egocentric photo-streams, *Pattern Recognition* 104 (2020) 107330. doi:10.1016/j.patcog.2020.107330.
- [6] M. Menchón, E. Talavera, J. Massa, P. Radeva, Behavioural patterns discovery for lifestyle analysis from egocentric photo-streams, *Pervasive and Mobile Computing* 95 (2023) 101846. doi:10.1016/j.pmcj.2023.101846.
- [7] M. Wang, J. Xing, Y. Liu, Actionclip: A new paradigm for video action recognition (2021). arXiv:2109.08472.
- [8] W. Wu, Z. Sun, W. Ouyang, Revisiting classifier: Transferring vision-language models for video recognition, in: *Proceedings of the AAAI Conference on Artificial Intelligence*, Vol. 37, 2023, pp. 2847–2855.
- [9] R. Dai, S. Das, K. Kahatapitiya, M. S. Ryoo, F. Brémond, Ms-tct: Multi-scale temporal convtransformer for action detection, in: *Proceedings of the IEEE/CVF Conference on Computer Vision and Pattern Recognition*, 2022, pp. 20041–20051.
- [10] R. Dai, S. Das, L. Minciullo, L. Garattoni, G. Francesca, F. Bremond, Pdan: Pyramid dilated attention network for action detection, in: *Proceedings of the IEEE/CVF Winter Conference on Applications of Computer Vision*, 2021, pp. 2970–2979.
- [11] X. Wang, S. Zhang, Z. Qing, Y. Shao, Z. Zuo, C. Gao, N. Sang, Oadtr: Online action detection with transformers, in: *ICCV*, 2021, pp. 7565–7575.
- [12] A. Ulhaq, N. Akhtar, G. Pogrebna, A. Mian, Vision transformers for action recognition: A survey, arXiv:2209.05700 (2022).

- [13] J. Chen, C. M. Ho, Mm-vit: Multi-modal video transformer for compressed video action recognition, in: Proceedings of the IEEE/CVF Winter Conference on Applications of Computer Vision (WACV), 2022, pp. 1910–1921.
- [14] J. Carreira, A. Zisserman, Quo vadis, action recognition? a new model and the kinetics dataset, in: 2017 IEEE Conference on Computer Vision and Pattern Recognition (CVPR), 2017, pp. 4724–4733. doi:10.1109/CVPR.2017.502.
- [15] M. Fayyaz, E. Bahrami, A. Diba, M. Noroozi, E. Adeli, L. V. Gool, J. Gall, 3d cnns with adaptive temporal feature resolutions, in: CVPR, 2021.
- [16] M. E. Kalfaoglu, S. Kalkan, A. A. Alatan, Late temporal modeling in 3d cnn architectures with bert for action recognition, in: Computer Vision – ECCV 2020 Workshops, 2020, pp. 731–747.
- [17] Z. Li, K. Gavriluk, E. Gavves, M. Jain, C. G. Snoek, Videolstm convolves, attends and flows for action recognition, Computer Vision and Image Understanding 166 (2018) 41–50. doi:10.1016/j.cviu.2017.10.011.
- [18] J.-Y. He, X. Wu, Z.-Q. Cheng, Z. Yuan, Y.-G. Jiang, Db-lstm: Densely-connected bi-directional lstm for human action recognition, Neurocomputing 444 (2021) 319–331.
- [19] J. An, H. Kang, S. H. Han, M.-H. Yang, S. J. Kim, Miniroad: Minimal rnn framework for online action detection, in: ICCV, 2023, pp. 10341–10350.
- [20] A. Vaswani, N. Shazeer, N. Parmar, J. Uszkoreit, L. Jones, A. N. Gomez, Ł. Kaiser, I. Polosukhin, Attention is all you need, Advances in neural information processing systems 30 (2017).
- [21] T. B. Brown, B. Mann, N. Ryder, et al., Language models are few-shot learners (2020). arXiv:2005.14165.
- [22] H. Touvron, L. Martin, K. Stone, et al., Llama 2: Open foundation and fine-tuned chat models (2023). arXiv:2307.09288.

- [23] J. Devlin, M.-W. Chang, K. Lee, K. Toutanova, Bert: Pre-training of deep bidirectional transformers for language understanding, arXiv:1810.04805 (2018).
- [24] A. Dubey, A. Jauhri, A. Pandey, A. Kadian, et al., The llama 3 herd of models (2024). arXiv:2407.21783.
URL <https://arxiv.org/abs/2407.21783>
- [25] V. Sanh, Distilbert, a distilled version of bert: Smaller, faster, cheaper and lighter, arXiv preprint arXiv:1910.01108 (2019).
- [26] D. Surís, R. Liu, C. Vondrick, Learning the predictability of the future, arXiv:2101.01600 (2021).
- [27] J.-A. Castro-Vargas, A. Garcia-Garcia, P. Martinez-Gonzalez, S. Oprea, J. Garcia-Rodriguez, Unsupervised hyperbolic action recognition, in: ROBOT2022, 2023, pp. 479–488.
- [28] O. Zatsarynna, J. Gall, Action anticipation with goal consistency, in: 2023 IEEE International Conference on Image Processing (ICIP), 2023, pp. 1630–1634. doi:10.1109/ICIP49359.2023.10222914.
- [29] Q. Zhao, S. Wang, C. Zhang, C. Fu, M. Q. Do, N. Agarwal, K. Lee, C. Sun, Antgpt: Can large language models help long-term action anticipation from videos?, ICLR (2024).
- [30] R. Dai, S. Das, S. Sharma, L. Minciullo, L. Garattoni, F. Bremond, G. Francesca, Toyota smarthome untrimmed: Real-world untrimmed videos for activity detection, TPAMI (2022) 1–1doi:10.1109/TPAMI.2022.3169976.
- [31] M. Benavent-Lledo, S. Oprea, J. A. Castro-Vargas, D. Mulero-Perez, J. Garcia-Rodriguez, Predicting human-object interactions in egocentric videos, in: 2022 International Joint Conference on Neural Networks (IJCNN), 2022, pp. 1–7. doi:10.1109/IJCNN55064.2022.9892910.
- [32] C. Feichtenhofer, H. Fan, J. Malik, K. He, Slowfast networks for video recognition, in: Proceedings of the IEEE/CVF International Conference on Computer Vision (ICCV), 2019.

- [33] A. Arnab, M. Dehghani, G. Heigold, C. Sun, M. Lučić, C. Schmid, Vivit: A video vision transformer, in: Proceedings of the IEEE/CVF international conference on computer vision, 2021, pp. 6836–6846.
- [34] G. Bertasius, H. Wang, L. Torresani, Is space-time attention all you need for video understanding?, in: Proceedings of the International Conference on Machine Learning (ICML), 2021.
- [35] Z. Liu, J. Ning, Y. Cao, Y. Wei, Z. Zhang, S. Lin, H. Hu, Video swin transformer, in: Proceedings of the IEEE/CVF conference on computer vision and pattern recognition, 2022, pp. 3202–3211.
- [36] Z. Liu, Y. Lin, Y. Cao, H. Hu, Y. Wei, Z. Zhang, S. Lin, B. Guo, Swin transformer: Hierarchical vision transformer using shifted windows, in: Proceedings of the IEEE/CVF International Conference on Computer Vision (ICCV), 2021, pp. 10012–10022.
- [37] H. Fan, B. Xiong, K. Mangalam, Y. Li, Z. Yan, J. Malik, C. Feichtenhofer, Multiscale vision transformers, in: ICCV, 2021.
- [38] Y. Li, C.-Y. Wu, H. Fan, K. Mangalam, B. Xiong, J. Malik, C. Feichtenhofer, Mvitv2: Improved multiscale vision transformers for classification and detection, in: CVPR, 2022.
- [39] J. Deng, W. Dong, R. Socher, L.-J. Li, K. Li, L. Fei-Fei, Imagenet: A large-scale hierarchical image database, in: 2009 IEEE Conference on Computer Vision and Pattern Recognition, 2009, pp. 248–255. doi: 10.1109/CVPR.2009.5206848.
- [40] J. Chalk, J. Huh, E. Kazakos, A. Zisserman, D. Damen, Tim: A time interval machine for audio-visual action recognition, arXiv:2404.05559 (2024).
- [41] A. Dosovitskiy, L. Beyer, A. Kolesnikov, D. Weissenborn, X. Zhai, T. Unterthiner, M. Dehghani, M. Minderer, G. Heigold, S. Gelly, et al., An image is worth 16x16 words: Transformers for image recognition at scale, arXiv:2010.11929 (2020).
- [42] W. Wu, Z. Sun, Y. Song, J. Wang, W. Ouyang, Transferring vision-language models for visual recognition: A classifier perspective, International Journal of Computer Vision (2023) 1–18.

- [43] K. He, X. Zhang, S. Ren, J. Sun, Deep residual learning for image recognition, in: Proceedings of the IEEE conference on computer vision and pattern recognition, 2016, pp. 770–778.
- [44] C. Szegedy, V. Vanhoucke, S. Ioffe, J. Shlens, Z. Wojna, Rethinking the inception architecture for computer vision, in: Proceedings of the IEEE conference on computer vision and pattern recognition, 2016, pp. 2818–2826.
- [45] Y. Ming, L. Xiong, X. Jia, Q. Zheng, J. Zhou, Fsconformer: A frequency-spatial-domain cnn-transformer two-stream network for compressed video action recognition, in: 2023 IEEE Smart World Congress (SWC), IEEE, 2023, pp. 838–843.
- [46] J. Wang, L. Torresani, Deformable video transformer, in: CVPR, 2022, pp. 14053–14062.
- [47] Y. Ming, J. Zhou, N. Hu, F. Feng, P. Zhao, B. Lyu, H. Yu, Action recognition in compressed domains: A survey, *Neurocomputing* 577 (2024) 127389. doi:10.1016/j.neucom.2024.127389.
- [48] S. Li, Z. Tao, K. Li, Y. Fu, Visual to text: Survey of image and video captioning, *IEEE Transactions on Emerging Topics in Computational Intelligence* 3 (4) (2019) 297–312. doi:10.1109/TETCI.2019.2892755.
- [49] A. Radford, J. W. Kim, C. Hallacy, A. Ramesh, G. Goh, S. Agarwal, G. Sastry, A. Askell, P. Mishkin, J. Clark, G. Krueger, I. Sutskever, Learning transferable visual models from natural language supervision (2021). [arXiv:2103.00020](https://arxiv.org/abs/2103.00020).
- [50] H. Xu, G. Ghosh, P.-Y. Huang, D. Okhonko, A. Aghajanyan, F. Metze, L. Zettlemoyer, C. Feichtenhofer, Videoclip: Contrastive pre-training for zero-shot video-text understanding, [arXiv:2109.14084](https://arxiv.org/abs/2109.14084) (2021).
- [51] W. Wu, X. Wang, H. Luo, J. Wang, Y. Yang, W. Ouyang, Bidirectional cross-modal knowledge exploration for video recognition with pre-trained vision-language models, in: Proceedings of the IEEE/CVF Conference on Computer Vision and Pattern Recognition, 2023.

- [52] A. Caesar, O. Özdemir, C. Weber, S. Wermter, Enabling action cross-modality for a pretrained large language model, *Natural Language Processing Journal* (2024) 100072doi:10.1016/j.nlp.2024.100072.
- [53] V. Manousaki, K. Bacharidis, K. Papoutsakis, A. Argyros, Vlmah: Visual-linguistic modeling of action history for effective action anticipation, in: *Proceedings of the IEEE/CVF International Conference on Computer Vision*, 2023, pp. 1917–1927.
- [54] A. Furnari, G. M. Farinella, Rolling-unrolling lstms for action anticipation from first-person video, *IEEE transactions on pattern analysis and machine intelligence* 43 (11) (2020) 4021–4036.
- [55] C. Zhang, C. Fu, S. Wang, N. Agarwal, K. Lee, C. Choi, C. Sun, Object-centric video representation for long-term action anticipation, in: *2024 IEEE/CVF Winter Conference on Applications of Computer Vision (WACV)*, 2024, pp. 6737–6747. doi:10.1109/WACV57701.2024.00661.
- [56] D. Shao, Y. Zhao, B. Dai, D. Lin, Finegym: A hierarchical video dataset for fine-grained action understanding, in: *IEEE Conference on Computer Vision and Pattern Recognition (CVPR)*, 2020.
- [57] N. Hussein, E. Gavves, A. W. Smeulders, Timeception for complex action recognition, in: *Proceedings of the IEEE/CVF Conference on Computer Vision and Pattern Recognition (CVPR)*, 2019.
- [58] X. Puig, K. Ra, M. Boben, J. Li, T. Wang, S. Fidler, A. Torralba, Virtualhome: Simulating household activities via programs, in: *Proceedings of the IEEE Conference on Computer Vision and Pattern Recognition*, 2018, pp. 8494–8502.
- [59] L. Beyer, X. Zhai, A. Kolesnikov, Better plain vit baselines for imagenet-1k (2022). [arXiv:2205.01580](https://arxiv.org/abs/2205.01580).
- [60] P. Xu, X. Zhu, D. A. Clifton, Multimodal learning with transformers: A survey, *IEEE Transactions on Pattern Analysis and Machine Intelligence* 45 (10) (2023) 12113–12132. doi:10.1109/TPAMI.2023.3275156.
- [61] S. Das, R. Dai, M. Koperski, L. Minciullo, L. Garattoni, F. Bremond, G. Francesca, Toyota smarthome: Real-world activities of daily living, in: *2019 IEEE/CVF International Conference on Computer Vision (ICCV)*, 2019, pp. 833–842. doi:10.1109/ICCV.2019.00092.

- [62] L. Wang, Y. Xiong, Z. Wang, Y. Qiao, D. Lin, X. Tang, L. Val Gool, Temporal segment networks: Towards good practices for deep action recognition, in: ECCV, 2016.
- [63] D. Tran, H. Wang, L. Torresani, J. Ray, Y. LeCun, M. Paluri, A closer look at spatiotemporal convolutions for action recognition, in: Proceedings of the IEEE Conference on Computer Vision and Pattern Recognition (CVPR), 2018.
- [64] C. Feichtenhofer, X3d: Expanding architectures for efficient video recognition, in: Proceedings of the IEEE/CVF Conference on Computer Vision and Pattern Recognition (CVPR), 2020.
- [65] S. Ioffe, C. Szegedy, Batch normalization: Accelerating deep network training by reducing internal covariate shift, in: International conference on machine learning, pmlr, 2015, pp. 448–456.